Molecular Biology of the Cell
Vol. 13, 854–865, March 2002

Endoplasmic Reticulum Dynamics, Inheritance, and Cytoskeletal Interactions in Budding Yeast[V]

K. L. Fehrenbacher, D. Davis, M. Wu, I. Boldogh, and Liza A. Pon*

Department of Anatomy and Cell Biology, Columbia University, College of Physicians and Surgeons, New York, New York 10032

Submitted April 17, 2001; Revised December 5, 2001; Accepted December 12, 2001
Monitoring Editor: Tim Stearns

The endoplasmic reticulum (ER) in *Saccharomyces cerevisiae* consists of a reticulum underlying the plasma membrane (cortical ER) and ER associated with the nuclear envelope (nuclear ER). We used a Sec63p-green fluorescent protein fusion protein to study motility events associated with inheritance of cortical ER and nuclear ER in living yeast cells. During M phase before nuclear migration, we observed thick, apparently rigid tubular extensions emanating from the nuclear ER that elongate, undergo sweeping motions along the cell cortex, and shorten. Two findings support a role for microtubules in this process. First, extension of tubular structures from the nuclear ER is inhibited by destabilization of microtubules. Second, astral microtubules, structures that undergo similar patterns of extension, cortical surveillance and retraction, colocalize with nuclear ER extensions. During S and G_2 phases of the cell cycle, we observed anchorage of the cortical ER at the site of bud emergence and apical bud growth. Thin tubules of the ER that extend from the anchored cortical ER display undulating, apparently random movement and move into the bud as it grows. Finally, we found that cortical ER morphology is sensitive to a filamentous actin–destabilizing drug, latrunculin-A, and to mutations in the actin-encoding *ACT1* gene. Our observations support 1) different mechanisms and cytoskeletal mediators for the inheritance of nuclear and cortical ER elements and 2) a mechanism for cortical ER inheritance that is cytoskeleton dependent but relies on anchorage, not directed movement.

INTRODUCTION

The endoplasmic reticulum (ER) of animal cells forms a network of interconnected membrane tubules and cisternae, which can extend from the outer nuclear envelope to the periphery of the cell. ER tubules are highly dynamic and consist of three morphologically distinct elements: linear tubules, polygonal reticuli, and triple junctions (Lee and Chen, 1988). Cell-free studies revealed that addition of cytosol to ER-derived vesicles promotes formation of a reticular ER network (Dreier and Rapoport, 2000). Although ER reticulum formation in vitro does not require microtubules, several findings support a role for microtubules in control of ER structure and organization in vivo. Early findings indicated that the ER colocalizes with microtubules and that long-term destabilization of microtubules in fibroblasts leads to retraction of the ER from the cell periphery toward the nucleus (Terasaki *et al.*, 1986; Lee and Chen, 1988). More recently, Waterman-Storer and Salmon (1998) showed that 1) extension of the ER toward the cell periphery occurs by plus-end–directed movement of the ER along microtubules and 2) ER tubules may be associated with the tip or the lateral surface of a dynamic microtubule.

In plants, ER dynamics are often actin based. Many light and electron microscopy (EM) studies showed colocalization of the ER with actin bundles and other elements of the actin cytoskeleton (Goosen-de Roo *et al.*, 1983; Lichtscheidl *et al.*, 1990; White *et al.*, 1994; Liebe and Menzel, 1995; Boevink *et al.*, 1998). Moreover, ER movement during cytoplasmic streaming occurs along actin cables in *Characea* algal cells (Kachar and Reese, 1988) and requires actin and myosin in *Vallisneria* mesophyll cells (Liebe and Menzel, 1995). Finally, stimulation of alfalfa roots with Nod factors results in rearrangement of actin filaments and ER and changes in cytoplasmic streaming, nuclear movements, and vacuolar shape (Allen and Bennett, 1996).

Immunofluorescence studies depict the *Saccharomyces cerevisiae* ER as a simple ring juxtaposed with the plasma membrane (cortical ER) and surrounding the nuclear envelope (nuclear ER; Rose *et al.*, 1989; Preuss *et al.*, 1991). Recent

Article published online ahead of print. Mol. Biol. Cell 10.1091/mbc.01–04–0184. Article and publication date are at www.molbiolcell.org/cgi/doi/10.1091/mbc. 01–04–0184.

[V] Online version of this article contains video material. Online version is available at www.molbiolcell.org.

* Corresponding author. E-mail address: lap5@columbia.edu.

Abbreviations used: DAPI, 4′,6-diamidino-2-phenylindole; DMSO, dimethyl sulfoxide; EM, electron microscopy; ER, endoplasmic reticulum; F-actin, filamentous actin; GFP, green fluorescent protein; Lat-A, latrunculin-A.

studies using Sec63p-green fluorescent protein (GFP) revealed that the cortical ER is a network of highly dynamic tubules that undergo ring closure and tubule-branching movements, similar to the mammalian peripheral ER (Prinz *et al.*, 2000). Although cortical ER and nuclear ER in *S. cerevisiae* are spatially distinct, both appear to function in protein trafficking. Freeze-substitution experiments have shown that yeast ER membranes next to the plasma membrane are associated with ribosomes (Baba and Osumi, 1987). In addition, immuno-EM revealed similar resident ER proteins in both cortical ER and nuclear ER (Preuss *et al.*, 1991). Finally, Rossanese *et al.* (1999) showed that Sec12p, a transitional ER marker protein that initiates the COPII vesicle assembly pathway in Golgi biogenesis, is localized throughout both nuclear ER and cortical ER.

Previous EM work and $DiOC_6$ (3,3′-dihexyloxacarbocyanine iodide) staining of yeast cells support the idea that the cortical ER accumulates at the new bud site and in small buds and is the first organelle to be inherited during S phase (Preuss *et al.*, 1991; Koning *et al.*, 1996). Recent studies showed that some, but not all, mutations in proteins that mediate protein translocation and homotypic ER fusion can alter cortical ER morphology and influence the efficiency of cortical ER inheritance (Prinz *et al.*, 2000). Here, we used a Sec63p-GFP fusion protein, a marker for the rough ER in budding yeast, to study cell cycle-associated motility events that may contribute to inheritance of cortical ER and nuclear ER and the role of the cytoskeleton in these processes.

MATERIALS AND METHODS

Yeast Media, Plasmids, and Strains

PTY22 (*MAT***a** *ade2, ura3-52, leu2-3,112*), a derivative of D273-10B, MSY202 (*MAT***a**/*MATα*, *his4-619/HIS4, trp1-1/TRP1, leu2-3112/LEU2, ura3-1/URA3, act1-3/act1-3*), and MSY106 (*MAT***a**/*α*, his4-619/his4-619) were the only strains used in this study. Yeast cell growth was carried out according to the method of Sherman (1991). ER was visualized in living cells by transforming PTY22 with the plasmid pJK59, which encodes Sec63p-GFP, a fusion of the S65T V163A mutant of GFP to the carboxy terminus under the *SEC63* promoter. pJK59 was constructed according to a previously described method (Prinz *et al.*, 2000). To view microtubules, PTY22 cells were transformed with the *Xba*I-digested integrating plasmid pTS988, carrying the *TUB1-GFP* gene fusion. The resulting integration encodes the Tub1p-GFP fusion protein under the control of the constituitive *TUB1* promoter, with a *LEU2*-selectable marker. PTY22 cells expressing Sec63p-GFP were grown at 30°C in synthetic complete medium that did not contain uracil and was supplemented with 4× adenine, or 80 μg/ml (synthetic complete medium − uracil + 4× adenine), to reduce autofluorescence of an adenine metabolic precursor in vacuoles. PTY22 cells expressing Tub1p-GFP were grown in synthetic complete medium − leucine + 4× adenine at 30°C. PTY22 cells containing both Sec63p-GFP and Tub1p-GFP were grown in synthetic complete medium − uracil, leucine + 4× adenine at 30°C.

Visualization of ER and Cytoskeleton in Live Cells

Cells expressing GFP (Sec63p-GFP and Tub1p-GFP) were grown to midlog phase and applied to the surface of a flat bed of solid medium consisting of 2% agarose in synthetic complete medium. Coverslips were placed on the surface of the medium pad and sealed with Valap (1:1:1, Vaseline:lanolin:paraffin) for long-term viewing without drying. Images were collected with an Axioplan II microscope (Carl Zeiss, Oberköchen, Germany) using a Plan-Apochromat 100×/1.4 N.A. objective lens and a cooled CCD camera (Orca-100; Hamamatsu Photonics, Bridgewater, NJ). Light output from the 100-W mercury arc lamp was controlled using a shutter driver (Uniblitz D122; Vincent Associates, Rochester, NY) and attenuated using neutral density filters (Omega Optical, Brattleboro, VT). IP Lab software (Scanalytics, Fairfax, VA) was used to control the shutter driver and capture images. Image enhancement and analysis were performed using the public domain program NIH Image 1.6 (National Institutes of Health, Bethesda, MD) and Adobe Photoshop 6.0 (Adobe Systems, Mountain View, CA).

Time-lapse images of GFP-labeled cells were obtained with 1-s exposures at 5-, 10-, 15-, 20-, or 30-s intervals for up to 122 min of real time. Where noted, images were acquired digitally with a spinning disk confocal microscope (Tran *et al.*, 1999). We used the CSU-10 confocal scanning unit head (Yokogawa Electric, Tokyo, Japan), attached to the C-mount video port on top of an E600fn upright microscope equipped with a Plan Apochromat 100×/1.4 N.A. DIC objective lens (Nikon, Melville, NY). An argon-krypton laser source with ~50 mW of power at 488-nm excitation illuminated the scanning unit through an optical fiber (Omnichrome, Chino, CA). Images were captured with an Orca-1 cooled CCD digital camera (Hamamatsu Photonics) using OpenLab software (Improvision, Lexington, MA) to control the camera and shutter.

Visualization of the ER and Cytoskeleton in Fixed Cells

ER was also visualized in fixed cells using Sec63p-GFP and indirect immunofluorescence. Antisera raised against Sec61p (Pilon *et al.*, 1998) and GFP were used to detect the translocon complex component in the ER and Sec63p-GFP, respectively. YL 1/2, a rat mAb raised against yeast tubulin (Kilmartin and Adams, 1984), was used to label microtubules. Cell fixation and staining by indirect immunofluorescence was carried out using a method described in a previous publication (Smith *et al.*, 1995). The actin cytoskeleton was visualized with Alexa 594 phalloidin (Molecular Probes, Eugene, OR), using a method previously described (Boldogh *et al.*, 1998).

The relationship between astral microtubules and nuclear ER extensions was determined using three-dimensional analysis of fixed and stained yeast cells. Optical sections were obtained at 200-nm intervals through the entire cell with an exposure time of 1200 ms for imaging Sec63p-GFP, 500 ms for microtubules, and 200 ms for 4′,6-diamidino-2-phenylindole (dihydrochloride, DAPI)-labeled DNA. Optical sectioning was performed using a piezo-electric focus motor mounted on the objective lens of the microscope (Polytech PI, Auburn, MA). Each z-series of Sec63p-GFP–expressing cells was subjected to digital deconvolution using Inovision software (Raleigh, NC) on a silicon graphics O_2 computer.

Destabilization of Microtubules and Microfilaments

For experiments with nocodazole (Sigma-Aldrich, St. Louis, MO), cultures were grown to midlog phase at 30°C. Cells were treated with 0.5% dimethyl sulfoxide (DMSO, control) or 0.5% DMSO containing nocodazole, at a final concentration of 20 μg/ml, from a 3.3 mg/ml stock. Nocodazole-treated and untreated cultures were then incubated at 30°C for 2 h. After 2 h, >80% of nocodazole-treated cells were large-budded with a single nucleus, as confirmed by DAPI, and contained small bars or small dots of microtubules, as confirmed by immunofluorescence (Figure 6).

Filamentous actin (F-actin) was destabilized by adding latrunculin-A (Lat-A) to 500 μl of Sec63p-GFP–expressing cells to a final concentration of 500 μM from a 50 mM stock in DMSO. For control incubations, an equivalent amount of Lat-A–free DMSO was used. Treated and untreated cells were then incubated for 15 min at room temperature. Depolymerization of all F-actin–containing structures in Lat-A–treated cells was confirmed by fixing cells and staining with Alexa-phalloidin.

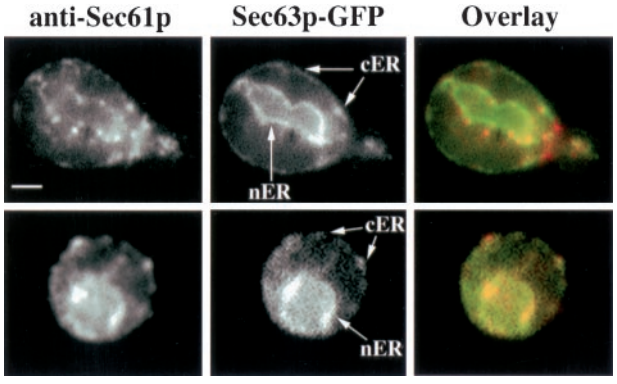

Figure 1. Sec63p-GFP is an accurate marker of the rough ER in *S. cerevisiae*. Wild-type cells (PTY22) expressing Sec63p-GFP (pJK59) were grown to midlog phase, fixed, and stained for Sec61p using indirect immunofluorescence, as described in MATERIALS AND METHODS. Cells were imaged in a single, central focal plane in the bud unless otherwise noted. Localization of Sec61p (left) and Sec63p-GFP (middle) and overlay showing the Sec61p and Sec63p-GFP (right) are shown in two representative cells (top and bottom). nER, nuclear envelope-associated ER; cER, cortical ER. Bar, 1 μm.

EM

Preparation of samples for transmission EM was carried out according to the methods of Stevens (1977). Yeast spheroplasts were fixed by addition of glutaraldehyde (Sigma-Aldrich) to growth medium to a final concentration of 5%. After incubation for 3 h at 23°C, cells were concentrated by centrifugation (10,000 $\times$ *g*, 10 min, room temperature) and washed two times with 0.9% NaCl. Samples were resuspended in 4% $KMnO_4$ in 0.1 M sodium cacodylate, pH 7.4 (Electron Microscopy Sciences, Fort Washington, PA), and incubated at 4°C for 1 h with gentle rotation. After two washes with 0.9% NaCl, samples were resuspended in 2% uranyl acetate (Electron Microscopy Sciences) and incubated for 1 h at 23°C. After three washes, the samples were dehydrated in a graded series of ethanol solutions, infiltrated with propylene oxide for 10 min, and embedded in Epon-812 (Tousimis Research, Rockville, MD). Ultrathin sections were stained for 5 min with 1% lead citrate before viewing with a 1200 transmission electron microscope (JEOL USA, Peabody, MA).

Velocity Measurements

Velocities of movements of ER tubules were determined from images recorded at 10-, 15-, or 20-s intervals. Velocity measurements were performed only on tubules undergoing linear, cortex-directed movement for at least three consecutive frames. For all velocity measurements, NIH Image 1.6 was used to determine the change in position (x and y coordinates) of the leading tip of each motile ER tubule during each time interval. These velocities were averaged to yield mean tubule velocity.

RESULTS

ER Morphology during Vegetative Growth

Sec63p is an essential component of the Sec complex, an ER membrane protein complex that associates with ribosomes and mediates translocation of proteins into and across ER membranes (Deshaies *et al.*, 1991; Brodsky *et al.*, 1993; Panzner *et al.*, 1995). Previous studies showed that Sec63p-GFP localizes to cortical ER, a reticulum underlying the plasma membrane, and nuclear ER, ER associated with the nuclear

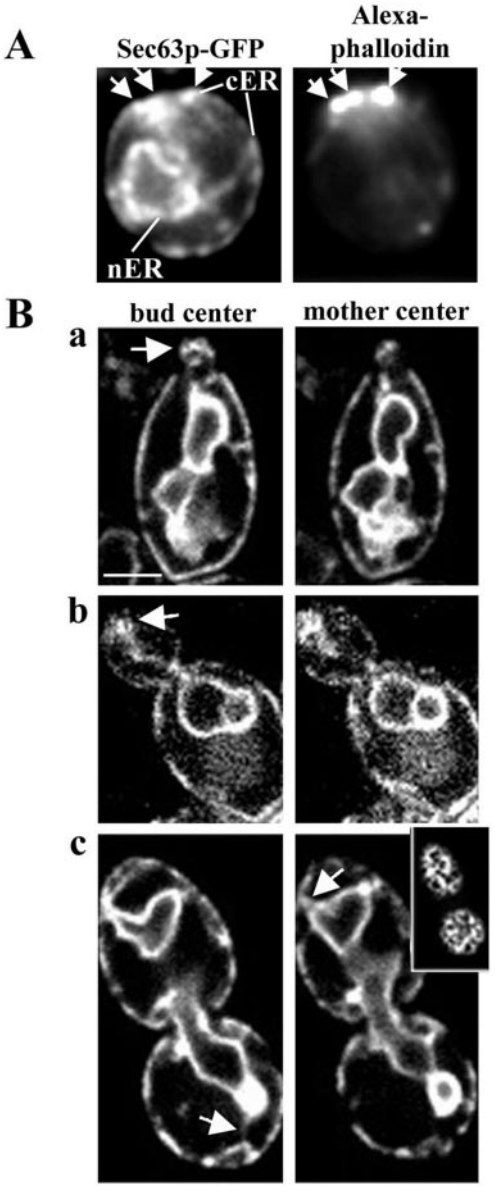

Figure 2. The cortical ER is enriched at the incipient bud site and in the small bud. (A) Cells expressing Sec63p-GFP were grown to midlog phase, fixed in formaldehyde, and stained with Alexa-phalloidin to visualize F-actin. Prebudded cells, with incipient bud sites marked by polarized actin patches, were imaged in a single, central focal plane. White arrows mark the position of the cortical ER (left) and the sites of actin patches at the incipient bud site (right). (B) Living cells expressing Sec63p-GFP. Cells were imaged in three dimensions with 0.3 μm between optical sections. Shown are optical sections through the center of the bud (left) and the center of the mother cell (right). Cells bearing small-sized (a), medium-sized (b), and large-sized (c) buds are shown. The inset image in c was obtained in the periphery of the cell. In a and b, white arrows mark the site of accumulation of cortical ER in the bud tip of cells in S-G_2 phase. (c) In large-budded cells, after nuclear migration, the cortical ER is more evenly distributed in the bud (top); however, ER tubules (white arrowheads) make multiple contacts with the cortex, especially at the bud tip and the tip of the mother cell distal to the bud. Images were obtained with the Yokogawa confocal microscope, as described in MATERIALS AND METHODS. Bar, 1 μm.

envelope. We expressed Sec63p-GFP in yeast using the construct prepared by J. Kahana (Prinz *et al.*, 2000). We confirmed that 1) expression of Sec63p-GFP has no obvious effect on cell viability, growth rates, or secretory function and 2) Sec63p-GFP is an accurate marker for rough ER. To evaluate Sec63p-GFP targeting, we compared its localization with that of endogenous Sec61p, a resident protein of the rough ER (Figure 1). Sec61p localizes to punctate structures at the cell cortex and on the nuclear envelope. At the cell cortex, Sec63p-GFP localized to punctate and linear structures that colocalized with Sec61p and uniformly stained the nuclear envelope. Because we expressed Sec63p-GFP in cells expressing endogenous Sec63p, it is possible that the GFP fusion protein localizes to some ER membranes outside of the Sec complex. In addition, we detected punctate structures using anti-Sec61p antibody that we did not detect with Sec63p-GFP. These instances were rare and may be due to loss of fluorescence from Sec63p-GFP upon fixation and preparation for antibody staining. Overall, our findings are consistent with previous reports that Sec63p-GFP is targeted to ER.

To deduce a pattern of ER inheritance, we imaged cells expressing Sec63p-GFP throughout the cell cycle (Figure 2). During the G_1 phase of the cell division cycle, a ring of actin patches accumulated at the presumptive bud site. We observed enrichment of cortical ER at the presumptive bud site and accumulation of cortical ER in the bud tip relative to other regions of the bud cortex in small- and medium-sized buds. Moreover, we detected thin ER tubules that extend from the bud tip to the nuclear ER and from the tip of the mother cell distal to the site of bud emergence to the nuclear ER. Both of these tubular connections between the cell cortex and nuclear ER align along the mother-bud axis. In late G_2 and M phases (large-budded cells), the cortical ER is more uniformly associated with the cortex of the bud, and numerous tubules are visible in both the mother and the daughter, reaching from the nuclear ER to the cortical ER. Quite often, however, these tubules were enriched at the tips of the bud and mother cell during the M phase.

Immobilization of the Cortical ER in the Bud Tip

Previous studies used time-lapse imaging to visualize cortical ER dynamics in vegetative yeast (Prinz *et al.*, 2000). In images obtained at 3-min intervals, these investigators observed dramatic rearrangement of the cortical ER in the bud. Using time-lapse imaging with greater temporal resolution, we studied the motility events that contribute to these rearrangements. Surprisingly, we did not detect any obvious polarized or linear movement of the cortical ER from mother cell to bud. Rather, we found that the cortical ER remained associated with the bud tip throughout the time of image analysis (>2 min) in cells bearing small-, medium-, and large-sized buds. Moreover, we found that tubules of the cortical ER extending from the bud tip along the mother-bud axis displayed undulations perpendicular to the mother-bud axis (Figure 3A). These observations suggest that the cortical ER may be retained in the bud by immobilization in the bud tip.

To test this hypothesis, we measured lateral movement of ER tubules emanating from the bud tip as a function of distance from the bud tip. If the cortical ER is immobilized in the bud tip, then extensions of the cortical ER adjacent to the site of immobilization should display less lateral movement than the cortical ER distal to the site of immobilization. By analogy, the distance of displacement of a vibrating guitar string will be shortest at the end, proximal to the bridge, and greatest at the center of the string. Indeed, we found that the

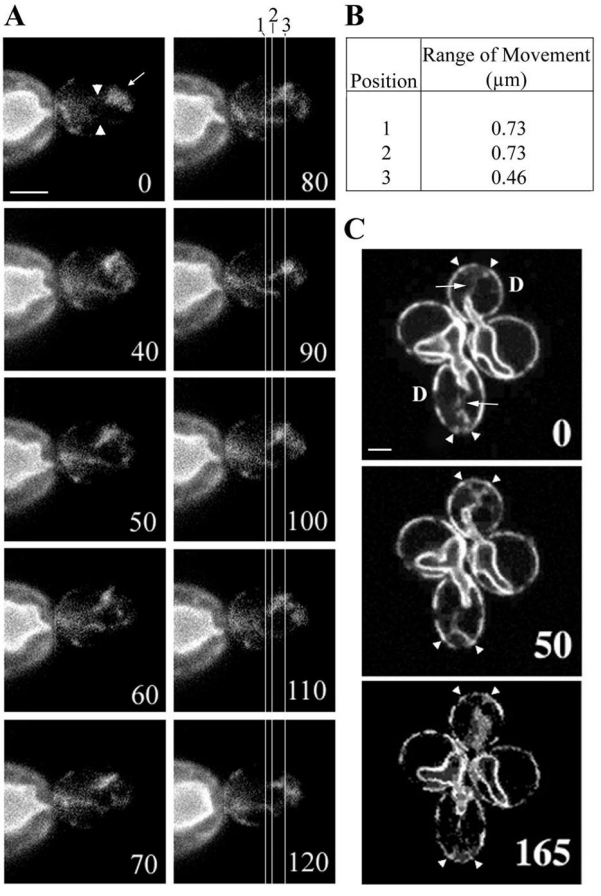

Figure 3. Time-lapse images of two types of ER tubule movement. Cells expressing Sec63p-GFP were grown in selective medium to midlog phase and imaged over time. Numbers at the lower right of each panel represent seconds elapsed in each experiment. (A) ER tubules in the small- to medium-sized bud (white arrowheads) are continuous with cortical ER enrichment at the bud tip and exhibit undulation while the ER at the tip remains immobilized (white arrow). During the period of imaging, the nuclear ER remained in the mother. (B) To quantify undulation, different points along the bud tip-bud neck axis were selected (labeled 1, 2, and 3 in A) and vertical axes were designated (white lines in A). Positions 1 and 2 represent regions in the center of the tubules between the two points of attachment: the nuclear ER (assumed, although resolution is limiting in the bud neck) and the cortical ER accumulation at the bud tip. Position 3 represents the point at which the two tubules contact the cortical ER in the bud tip. Distances between these tubules at the three different positions were recorded at each interval over the imaging period, and the maximum minus minimum distances were calculated as range of movement at each position. (C) ER tubules (white arrow) in a large-budded cell remain in contact with the cortical ER at the bud tip at fixed points (white arrowheads) in both daughter cells, "D," for >2 min. In all cases, analysis was restricted to the cortical ER that was visible in a single focal plane throughout the time of study. Bar, 1 μm.

average lateral displacement of ER tubules adjacent to the bud tip was half as great as the lateral displacement of ER tubules farther from the bud tip (Figure 3B). At the light microscopy level, no contact was observed between the lateral walls of the bud and the ER tubules; therefore, we conclude that the predominant restrictive forces on these tubules must be at the bud tip or at the point of connection with the nuclear ER and the nuclear envelope. This finding, together with the absence of any obvious linear, polarized, bud-directed cortical ER movement, suggests that cortical ER inheritance does not occur by active transport of the cortical ER from the mother cell to the bud. Rather, the cortical ER appears to be immobilized in the bud tip. Because the cortical ER is a reticular network, immobilization of part of the network may serve to draw the cortical ER into the bud as it grows.

The Actin Cytoskeleton Is Required for Normal Cortical ER Morphology

As described above, we observed enrichment and immobilization of the cortical ER at the presumptive bud site and in the bud tip relative to other regions of the bud cortex during apical bud growth. Although actin patches are also enriched at these sites (Figure 4), we did not detect any obvious colocalization of the cortical ER with actin patches. Moreover, in agreement with previously reported results (Prinz *et al.*, 2000), we did not observe significant colocalization between actin cables and the cortical ER.

Although there is no obvious coincidence between the cortical ER and major actin-containing structures in yeast, we found that perturbation of the actin cytoskeleton resulted in defects in the cortical ER morphology and localization. Comparison of wild-type and *act1-3* mutant cells by EM revealed the cortical ER as electron-dense, linear segments of membrane, juxtaposed to the plasma membrane (Figure 5). We found that ER structures in early stages of the cell cycle are more sensitive to destabilization of the actin cytoskeleton (see below). Therefore, we compared cortical ER segment length in ultrathin sections of wild-type and mutant yeast during the S-G_2 phase, i.e., in budded cells containing a premigratory nuclear envelope visible in the plane of section. In wild-type cells, the length of the continuous cortical ER membranes resolved in a single section was 0.37 μm (n = 141, SEM = 0.019). In contrast, the cortical ER membrane of the *act1-3* mutant exhibited aberrant morphology at semipermissive temperatures: the average length of a single continuous cortical ER membrane resolved within a single section was 0.16 μm (n = 193, SEM = 0.007; $p < 0.001$). Although it is not clear whether this change resulted from fragmentation of the cortical ER or from a change in the cortical ER position, it is clear that mutation of the actin-encoding *ACT1* gene affects cortical ER morphology.

Disrupting the F-actin cytoskeleton with the actin inhibitor, Lat-A (Ayscough *et al.*, 1997), also resulted in defects in the ER (Figure 6A). Approximately 80% of a heterogeneous population of cells exhibited a diffuse distribution of ER in the cytoplasm and a failure of the cortical ER to accumulate in the bud tip after short-term treatment with Lat-A (Figure 6B). The time of onset of these defects in the ER structure and localization correlates with that of Lat-A–induced actin destabilization. These findings are consistent with the previous report that short-term treatment with Lat-A results in a reduction in cortical ER dynamics in the bud (Prinz *et al.*, 2000).

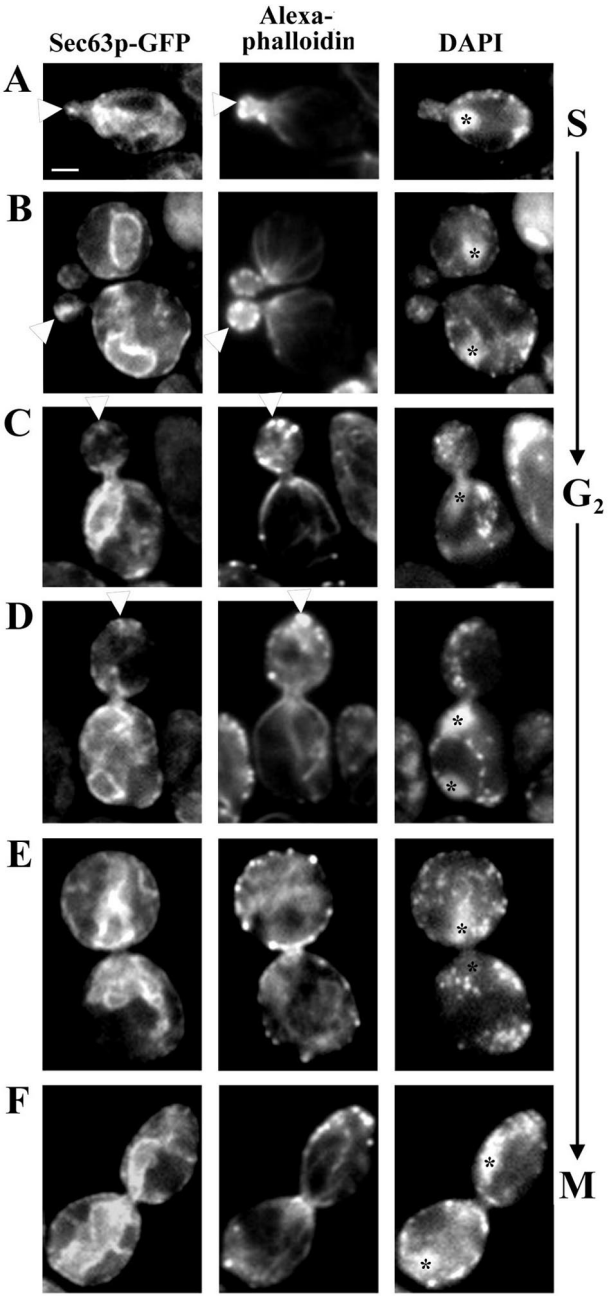

Figure 4. Sec63p-GFP-labeled ER displays a polarized pattern of inheritance. Cells expressing Sec63p-GFP were grown to midlog phase, fixed in formaldehyde and stained with both Alexa-phalloidin, to visualize F-actin, and DAPI, to visualize DNA. Cells were then imaged in a single, central focal plane of the bud. (A) The cortical ER is inherited early in S phase and enriched at sites of apical bud growth, coincident with actin patches (white arrowheads). (B–D) The cortical ER and actin patches are enriched in the bud tip during apical growth (white arrowheads). (E and F) Both actin patches and cortical ER are distributed at the cortex of a bud during late stages of the cell cycle. The asterisks denote the positions of nuclear DNA, by DAPI staining, including that which may be out of the plane of focus.

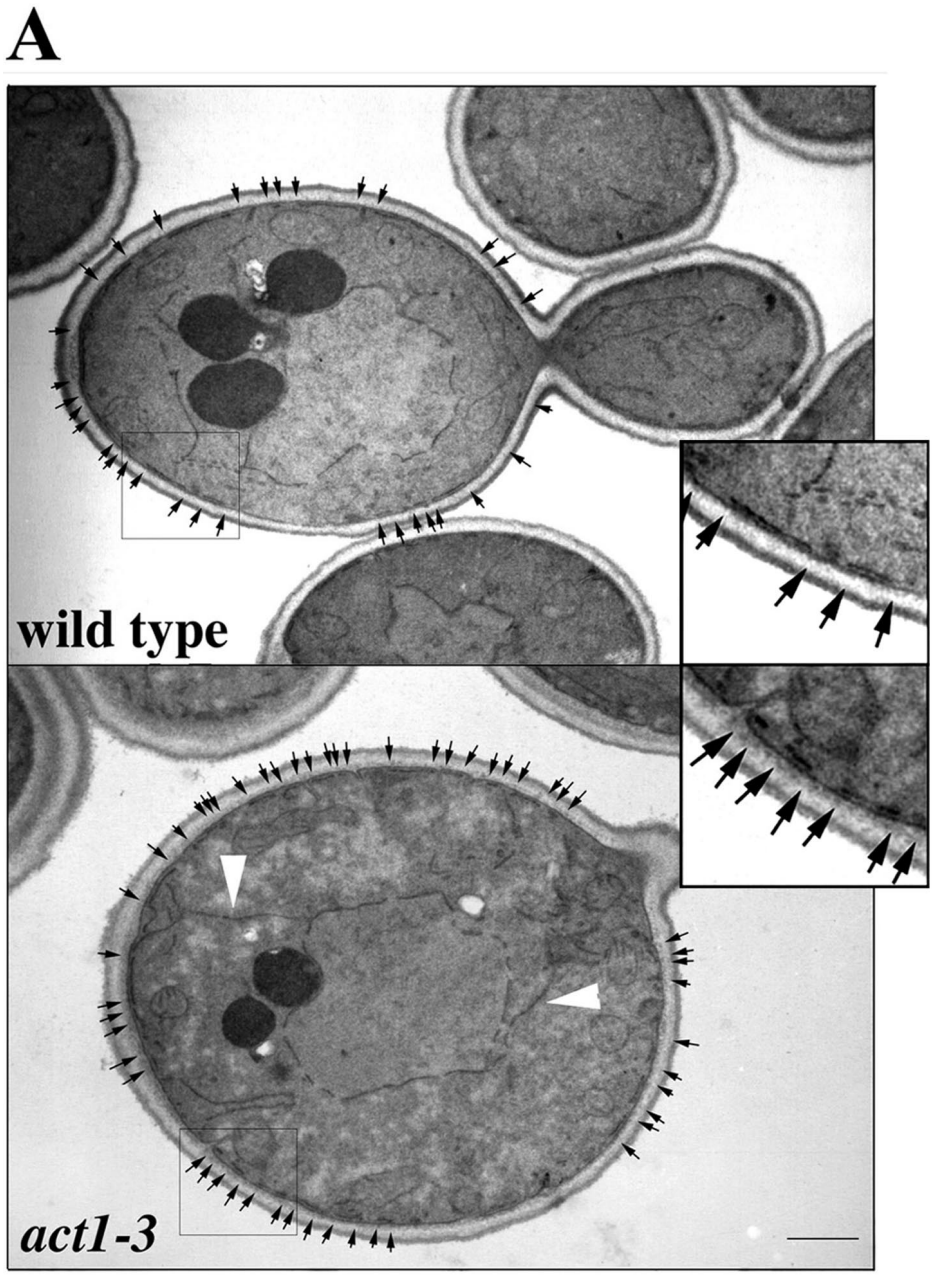

Figure 5. Cortical ER membranes exhibit an altered pattern in an *act1-3* mutant. In one EM optical section, the cortical ER appears as a linear membrane, juxtaposed to the plasma membrane. In wild-type cells (MSY106), cortical ER membranes in one thin section were approximately twice as long as those observed in *act1-3* mutant cells (MSY202). Insets show twofold enlargement of boxed cortex regions. Black arrows delineate the ends, or interruptions, in the cortical ER membrane. White arrowheads show cortical ER membranes, which connect the nuclear ER and the cortical ER at the distal tip of the mother and the bud site. Bar, 1 μm.

Finally, we observed that the cortical ER was most sensitive to Lat-A during apical bud growth, a stage in the yeast cell cycle when the cortical ER and actin patches are enriched at sites of polarized secretion. Cortical ER morphology defects occurred in 87 and 91% of cells bearing small- and medium-sized buds, respectively. In contrast, only 40% of large-budded cells showed ER morphology defects upon Lat-A treatment.

Dynamics of Tubular Extensions from the Nuclear ER

We observed a novel nuclear ER motility event during the G_2 to M phase transition. Using time-lapse fluorescence microscopy, we observed ER tubules extending from the nuclear ER into the bud (Figure 7). These tubules extended

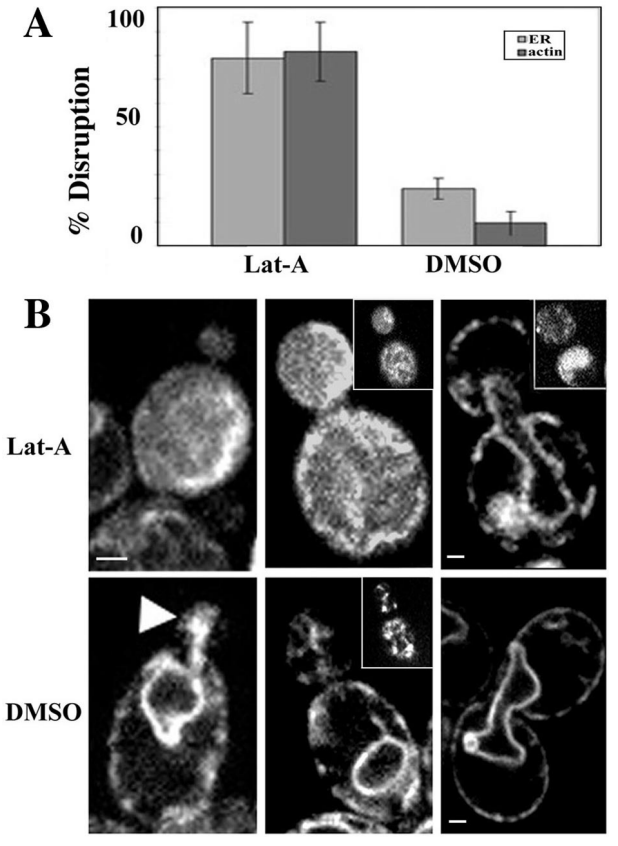

Figure 6. F-actin is required for normal cortical ER morphology in the bud. After 15 min of treatment with 500 μM Lat-A or DMSO, cells expressing Sec63p-GFP were fixed in formaldehyde and stained with Alexa-phalloidin. (A) In Lat-A–treated cells (B, top), the number of cells displaying normal ER morphology was reduced by 55%, compared with cells treated with DMSO only (B, bottom). (B) Lat-A-treated cells were then imaged in the central focal plane of the bud. Panels, from left to right, represent small-, medium-, and large-budded cells, respectively. The white arrowhead marks normal cortical ER enrichment in a small bud of a DMSO-treated, control cell. Insets in the middle panels show images at the periphery of corresponding cells. Top, right, large-budded cells, treated with Lat-A, with normal ER morphology. Inset in top, right, a cell with abnormal ER distribution. Images were obtained with Yokogawa confocal microscope as described in MATERIALS AND METHODS. Bar, 1 μm.

from nuclear ER at a rate of 2.62 $\pm$ 0.81 μm/min (n = 15) and made contact with the cortex of the bud. After initial cortical contact at the bud tip, the nuclear ER tubules exhibited "sweeping" motions along the cell cortex. Finally, after brief contact (66 $\pm$ 10.6 s; n = 15) with the cortex and cortical sweeping, the ER tubules shortened at a rate of 1.7 $\pm$ 0.47 μm/min (n = 5) back to the nuclear envelope. Unlike the thin, undulating cortical ER tubules that are anchored at the bud tip, tubules that extend from the nuclear ER to the cortex are thick and relatively rigid and did not display obvious undulating motion. Rather, they extended and shortened in a linear, seemingly track-dependent manner.

During anaphase B in yeast, the spindle is aligned along the mother-bud axis and elongates at a rate of 1.08 $\pm$ 0.31 μm/min (Yeh *et al.*, 1995). This spindle elongation drives elongation of the nucleus and movement of the nucleus from the mother cell into the bud (Shaw *et al.*, 1998). There are some similarities between nuclear migration during anaphase B and extension of tubular structures from the nuclear ER. Both processes result in the elongation of some or all of the nuclear envelope and extension of the elongated structure from the mother cell into the bud. Moreover, both processes depend on microtubules (see below). However, two lines of evidence indicate that the tubular extensions of the nuclear ER detected here are not a consequence of spindle-driven nuclear elongation and migration. First, the bulk of nuclear DNA is always in close proximity to the spindle pole and the leading edge of the nucleus during migration into the bud (Yeh *et al.*, 1995). In contrast, the tubular extension from the nuclear ER did not contain detectable DNA (Figure 8C, a and e). Second, the cortical sweeping motion detected in tubular structures extending from the nuclear ER has not been observed during nuclear migration. Thus, the pattern of movement of the nucleus during these two processes is different.

Role of Astral Microtubules in Extension of Tubular Structures from the Nuclear ER

Treatment of cells expressing Sec63p-GFP with the microtubule-destabilizing agent nocodazole resulted in reduction of spindle microtubules to a small bar and loss of all detectable cytoplasmic microtubules and nuclear migration in 81.5 $\pm$ 4% of cells examined. Loss of microtubules was confirmed by immunofluorescence and visualization of microtubules in live cells, using the tubulin fusion protein, Tub1p-GFP (Fehrenbacher, Davis, Wu, Boldogh, and Pon, unpublished results). The cortical ER remained intact and polarized in cells at all stages in the cell cycle after microtubule destabilization, suggesting that microtubules are necessary neither for the maintenance of the cortical reticulum nor for the polarized arrangement of the cortical ER during G_1-G_2 phases of the cell cycle (Figure 8A). However, destabilization of microtubules inhibited elongation of tubules from the nuclear ER. Specifically, we observed tubular extensions of the nuclear ER in 68 $\pm$ 5.7% of all large buds in G_2 to M phase yeast cells (n $>$ 200). In contrast, only 12 $\pm$ 4.7% of nocodazole-treated G_2 to M phase cells showed obvious tubular extensions of the nuclear ER (n $>$ 200; Figure 8B).

Consistent with this, three additional findings support a role for astral microtubules in tubular extension and movement of nuclear ER. First, the pattern of movement of nuclear ER extensions is similar to that of astral microtubules. Both astral microtubules and nuclear ER extensions display extension retraction and cortical sweeping motions (Carminati and Stearns, 1997). Second, the velocity for nuclear ER extension and retraction measured in this study is within the range of published velocities for astral microtubule extension and retraction (Tirnauer *et al.*, 1999). Third, we observed colocalization of astral microtubules and tubular extensions from the nuclear ER. Fourteen percent of the cells showed nuclear ER extensions in the absence of a detectable astral microtubule, and only 5% of cells contained an astral microtubule with no associated nuclear ER extension in the bud. However, 81% of G_2-M phase cells exhibited interaction of nuclear ER extension with some part of an astral microtubule (n = 127). Under conditions where the entire length of

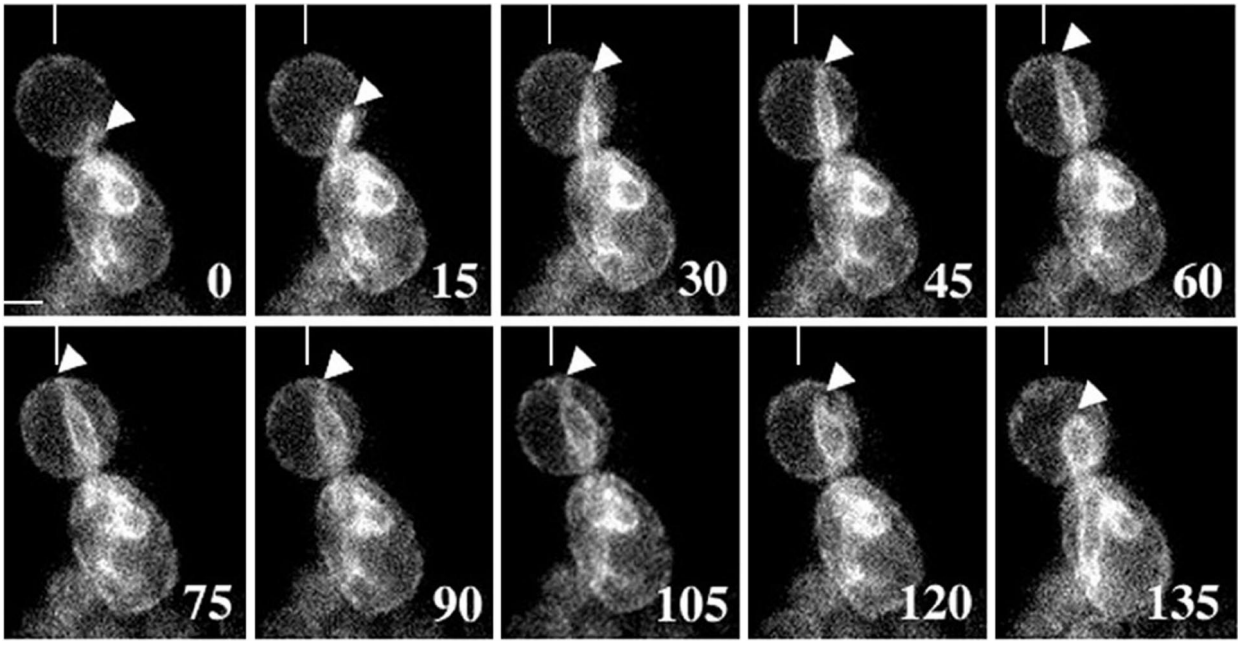

Figure 7. Extension of the ER from the nucleus to the cell cortex. An ER tubule (tip marked by white arrowhead), extending from the nuclear ER, exhibits a linear, cortex-directed movement. The ER tubule maintained cortical contact for <2 min in medium- to large-budded cells, moved along the cortex (sweeping), and retracted. Cells were imaged in the central focal plane of the bud. Numbers at the lower right of each panel represent seconds elapsed in each experiment. A vertical white line in the top of each panel provides a reference point for cortical sweeping. Bar, 1 μm.

a nuclear ER-associated astral microtubule was resolved in a single focal plane, 94% of cells showed coalignment of the astral microtubule along the entire lateral surface of the nuclear ER extension (n = 39; see Figure 8C). These data suggest that extension of the nuclear ER into the bud in G_2-M phase may depend on the dynamics of astral microtubules.

DISCUSSION

Partitioning of most organelles to the bud in *S. cerevisiae* is an active process that uses the cytoskeleton as tracks for movement. For instance, a type V myosin, Myo2p, is required for transfer of vacuoles into the bud during mitosis and movement to areas of polarized growth (Hill *et al.*, 1996; Catlett *et al.*, 1998). Although the Arp2/3 complex has been implicated as the force generator for transfer of mitochondria from mother cell to bud, this inheritance process also uses actin cables as tracks for movement (Simon *et al.*, 1995, 1997; Smith *et al.*, 1995; Boldogh *et al.*, 1998, 2001). Finally, nuclear migration in yeast is driven by microtubule dynamics and microtubule-dependent motor molecules (Palmer *et al.*, 1992; Sullivan and Huffaker, 1992; Eshel *et al.*, 1993; Li *et al.*, 1993).

Here, we propose a mechanism for cortical ER inheritance that is distinct from the inheritance of the nuclear ER and other organelles in budding yeast (Figure 9). We did not detect any obvious polarized or linear movement of the cortical ER from the mother cell to the bud. Moreover, there is no significant colocalization of the cortical ER with either microtubules or elements of the actin cytoskeleton. Rather, we found that the cortical ER is immobilized and enriched in the presumptive bud site and bud tip. This immobilization began in G_1 and early S phase. As a result, the cortical ER was enriched at the incipient bud site and was present in the new bud as soon as it emerged. Immobilization of the cortical ER in the bud tip persisted as the bud grew through late S and G_2 phase.

We propose that immobilization of the cortical ER at the bud tip serves two important functions. The first is to ensure that the cortical ER is transferred to the bud. This mechanism of inheritance may be optimal for the cortical ER, because the cortical ER has a different morphology compared with other organelles. In contrast to other organelles or particles that are discontinuous (e.g., secretory vesicles), or large and require significant levels of force for movement (e.g., nucleus, mitochondria, and vacuoles), the cortical ER consists of tubules of small diameter that form a continuous reticulum. As a result, anchorage of part of the cortical ER results in the pulling of some of the network into the bud as it enlarges.

The second is to localize the machinery for protein synthesis and secretion to the site of polarized cell surface growth. It is clear that actin cables are used as tracks for transport of vesicles and Sec4p, a protein required for secretion, from the mother cell to the bud (Finger and Novick, 1998). However, pulse-chase studies showed that inhibition of Myo2p, the motor for actin-based vesicular movement, had no obvious effect on polarized delivery of some secretory and vacuolar proteins to the bud (Govindan *et al.*, 1995). Moreover, other studies showed that mRNA of *ASH1*, a

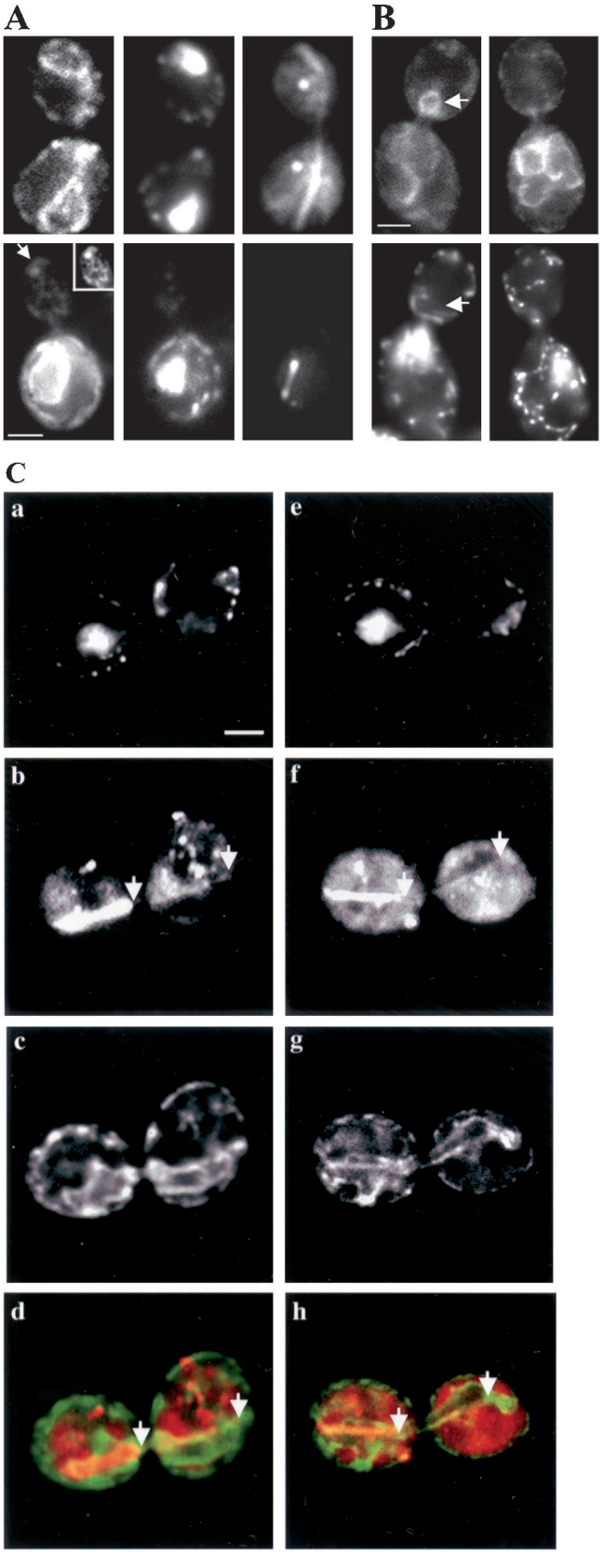

gene required in mating-type determination in yeast, is transported to and accumulates in the bud tip (Takizawa *et al.*, 1997; Beach *et al.*, 1999). Our observation that the rough ER is immobilized in the bud tip raises the possibility that it may contribute to 1) localization of the machinery for protein secretion to sites of polarized membrane deposition and 2) localization and synthesis of Golgi elements at that site.

Previous studies showed that mitochondria are immobilized in the bud tip and in the tip of the mother cell distal to the site of bud emergence (Yang *et al.*, 1999). We see an enrichment of the cortical ER at sites of retention of mitochondria in dividing yeast. Therefore, it is possible that these immobilization events are mediated by the same molecules or respond to similar cellular cues. Indeed, other studies indicated that mutations that affect the cortical ER morphology also affect mitochondrial morphology (Prinz *et al.*, 2000). Consistent with this, the cortical ER, like mitochondria, depend on the actin cytoskeleton.

Previous studies indicated that short-term treatment of yeast with an actin-destabilizing agent results in a change in the cortical ER dynamics in the bud (Prinz *et al.*, 2000). We confirmed this observation and showed that cells undergoing apical bud growth are more sensitive to Lat-A–dependent ER destabilization than cells at later stages in the cell division cycle. Although it is not clear whether the cortical ER and the actin cytoskeleton interact directly, these findings support 1) a role for the actin cytoskeleton in control of ER morphology and inheritance and 2) a cell cycle dependence of actin-cortical ER interactions. Finally, our findings

Figure 8. Microtubules are required for extension of the nuclear ER but not the normal cortical ER morphology. (A) Depolymerization of microtubules after nocodazole treatment yields no significant effect on the cortical and nuclear distribution of ER in the mother cell and the bud. Cells expressing Sec63p-GFP were incubated with DMSO alone (top) or 20 μg/ml nocodazole in DMSO (bottom), then fixed, and spheroplasted after 2 h. The ER and microtubules were detected using Sec63p-GFP and antibodies to GFP (left) or antibodies to tubulin, YL 1/2 (right). DAPI staining is shown in the middle. The white arrow (bottom, left) marks the cortical ER in the bud tip. The inset shows enhanced region of interest in the same section of the bud. (B) Nocodazole treatment blocks extensions of the nuclear ER into the bud. Cells expressing Sec63p-GFP were incubated with DMSO alone (left) or 20 μg/ml nocodazole in DMSO (right). After 2 h, cells were fixed and viewed. The white arrow marks the position of the nuclear ER extension in the corresponding GFP and DAPI channels (top and bottom left). Note the absence of nuclear DNA in or near the nuclear ER extension. In A and B, cells were imaged in the central focal plane of the bud. Bar, 1 μm. (C) Astral microtubules associate along the lateral edge of nuclear ER extensions. Cells expressing Sec63p-GFP were fixed, converted to spheroplasts, and stained with DAPI to visualize DNA (a and e) and antibodies against tubulin (b and f) and GFP (c and g). For imaging, optical sections were obtained through the entire depth of the cell, and images were enhanced by digital deconvolution. Single focal planes containing the full length of the astral microtubule are shown. The white arrows mark the ends of the astral microtubule. Overlays of the tubulin (red) and GFP (green) staining show alignment of astral microtubules along the lateral surface of the nuclear ER extensions (d and h). Nuclear ER extensions do not contain DNA (a and e). Cells were overexposed to reveal the less intense antitubulin staining of the astral microtubule; therefore, the spindle is not well resolved. Bar, 1 μm.

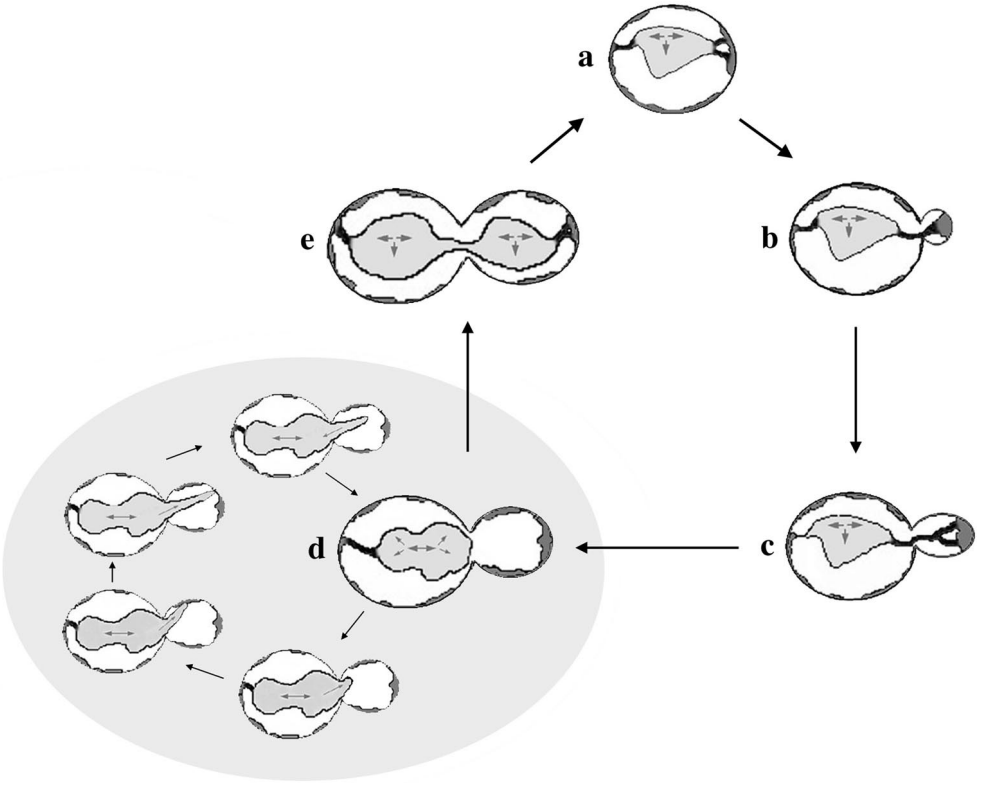

Figure 9. Model of ER inheritance in budding yeast. Schematic diagram depicting a model for ER inheritance during the cell cycle of *S. cerevisiae*. The cortical ER is depicted in dark gray, and nonmotile tubules extending from the nuclear ER to the cortical ER are depicted in black. The nuclear ER is depicted in light gray. (a) The cortical ER enriches at the presumptive bud site, coincident with enrichment of F-actin in unbudded, but polarized, cells in early S phase. The nuclear ER in the mother maintains a connection to the distal tip cortex throughout the entire cell cycle. (b) As a small bud is formed, the cortical ER remains enriched in the bud tip. (c) During apical bud growth, the cortical ER remains enriched and immobilized in the bud tip, whereas the ER tubules extending from the enrichment undulate and exhibit undirected movement. (d) As G_2/M phase begins, the nucleus and the nuclear ER are positioned at the bud neck, spindle microtubules begin elongating along the mother-daughter axis, and the cortical ER in the bud is more evenly distributed, concurrent with the end of apical growth of the bud. At this stage, before nuclear migration into the bud, tubular extensions emanating from the leading edge of the nuclear ER rapidly elongate in a linear, bud-tip direction, contact the bud tip cortex for <2 min, exhibit sweeping motions, and then retract in a linear manner. Results from this study suggest that these nuclear ER extensions are astral-microtubule dependent. (e) At the end of the M phase, nuclear ER tubules exhibit long-term contact with the cortex at the distal tip of the mother and the bud tip. Gray single-headed arrows represent directional movements of astral microtubules, emanating from the spindle pole body. Gray double-headed arrows represent the direction of spindle elongation.

indicate that cortical ER inheritance has a different cytoskeleton dependence compared with the nuclear ER.

Finally, we observed extension and retraction of tubular structures from the nuclear ER to the cell cortex. During late mitosis, tubules emanating from the nuclear ER exhibit linear, cortex-directed movement and sweeping motions when in contact with the cortex/cortical ER. These tubules make transient associations with the cortex (<2 min) and make most of their contacts at the bud tip. The dynamic extensions of the nuclear ER, documented in this study (Figure 7), are not produced by nuclear migration during anaphase B, because tubular extensions from the nuclear ER contain no nuclear DNA (Figure 8, B and C) and show a pattern of movement that is distinct from that of the nucleus during migration from the mother cell to the bud. Nuclear ER extensions colocalize with astral microtubules and are sensitive to a microtubule-destabilizing agent. Specifically, our three-dimensional data suggest that the majority of astral microtubules associate along the entire lateral surface of the nuclear ER extensions. These observations support a role for astral microtubules in extension, retraction, and cortical sweeping by nuclear ER extensions.

These findings are important for three reasons. First, recent studies supported the role of astral microtubules in cortical surveillance, proper alignment of the spindle, and establishing the polarity of nuclear migration during mitosis in budding yeast (Carminati and Stearns, 1997; Shaw *et al.*, 1997). Our finding indicates that the nuclear ER may also contribute to this process. Second, the microtubule association and pattern of movement displayed by tubular extensions of the nuclear ER are similar to those described for peripheral ER tubules in animal cells (Waterman-Storer and Salmon, 1998). In animal cells, this process may occur by plus-end–directed movement along microtubules or by association of ER with a dynamic microtubule. Our finding that a similar process may occur in yeast provides additional support for the notion that the ER in yeast is similar to that of other eukaryotes. Third, although the cortical ER and the nuclear ER are spatially distinct, these structures have similar functions and are linked by thin tubular connections. These tubular connections maintain long-term associations (>2 min) to the cortical ER at fixed points, usually at the cortex of the bud tip, and exhibit undulation (Figure 3C). Because tubular extensions of the nuclear ER extend to and

retract from the cell cortex, it is possible that these extensions from the nuclear ER mediate communication and/or exchange of material between the cortical ER and the nuclear ER. Ongoing studies are designed to explore these issues.

ACKNOWLEDGMENTS

We thank Dr. F. Chang (Columbia University, New York) for use of the Yokogawa confocal microscope; Dr. P. Tran (Columbia University) for invaluable microscopy training and support; members of the Pon laboratory for their critical expertise and support; T. Swayne and S. Swamy for support in the Optical Imaging Facility of the Herbert Irving Comprehensive Cancer Center; H. O'Sullivan for EM; Dr. P. Crews for supplying us with Lat-A; and A. Palazzo and the Gundersen laboratory (Columbia University) for sharing nocodazole and YL 1/2. PTY22 was generously provided by P. Thorsness (University of Wyoming, Laramie, WY). pJK59 was constructed by J. Kahana (University of California, San Diego, La Jolla, CA) and kindly provided by the laboratory of Dr. P. Silver, along with GFP antibody (Harvard Medical School, Boston, MA). pTS988 was very generously provided by Dr. T. Stearns (Stanford University, Stanford, CA). This work was supported by research grants to L.P. from the National Institutes of Health (GM-45735) and the American Cancer Society (RPG-97-163-04-CSM) and by a training grant to K.F. from the National Institutes of Health (T32 NS-07430).

REFERENCES

Allen, N.S., and Bennett, M.N. (1996). Electro-optical imaging of F-actin and endoplasmic reticulum in living and fixed plant cells. Scanning Microsc. Suppl. *10*, 177–186.

Ayscough, K.R., J. Stryker, N. Pokala, M. Sanders, P. Crews, and Drubin, D.G. (1997). High rates of actin filament turnover in budding yeast and roles for actin in establishment and maintenance of cell polarity revealed using the actin inhibitor latrunculin-A. J. Cell Biol. *137*, 399–416.

Baba, M., and Osumi, M. (1987). Transmission and scanning electron microscopy examination of intracellular organelles in freeze-substituted *Kloeckera* and *Saccharomyces cerevisiae* yeast cells. J. Electron Microsc. Technol. *5*, 249–261.

Beach, D.L., Salmon, E.D., and Bloom, K. (1999). Localization and anchoring of mRNA in budding yeast. Curr. Biol. *9*, 569–578.

Boevink, P., Oparka, K., Santa Cruz, S., Martin, B., Betteridge, A., and Hawes, C. (1998). Stacks on tracks: the plant Golgi apparatus traffics on an actin/ER network. Plant J. *15*, 441–447.

Boldogh, I., Vojtov, N., Karmon, S.L., and Pon, L.A. (1998). Interaction between mitochondria and the actin cytoskeleton in budding yeast requires two integral mitochondrial outer membrane proteins, Mmm1p and Mdm10p. J. Cell Biol.*141*, 1371–1391.

Boldogh, I., Yang, H.C., Nowakowski, W.D., Karmon, S.L., Hays, L.G., Yates, J.R., and Pon, L.A. (2001). Arp2/3 complex and actin dynamics are required for actin-based mitochondrial motility in yeast. Proc. Natl. Acad. Sci. USA *98*, 3162–3167.

Brodsky, J.L., Hamamoto, S., Feldheim, D., and Schekman, R. (1993). Reconstitution of protein translocation from solubilized yeast membranes reveals topologically distinct roles for BiP and cytosolic Hsc70. J. Cell Biol. *120*, 95–102.

Carminati, J.L., and Stearns, T. (1997). Microtubules orient the mitotic spindle in yeast through dynein-dependent interactions with the cell cortex. J. Cell Biol. *138*, 629–641.

Catlett, N.L., and Weisman, L.S. (1998). The terminal tail region of a yeast myosin-V mediates its attachment to vacuole membranes and sites of polarized growth. Proc. Natl. Acad. Sci. USA *95*, 14799–14804.

Deshaies, R.J., Sanders, S.L., Feldman, D.A., and Schekman, R. (1991). Assembly of yeast Sec proteins involved in translocation into the endoplasmic reticulum into a membrane-bound multisubunit complex. Nature *349*, 806–808.

Dreier, L., and Rapoport, T.A. (2000). In vitro formation of the endoplasmic reticulum occurs independently of microtubules by a controlled fusion reaction. J. Cell Biol. *148*, 883–898.

Eshel, D., Urrestarazu, L.A., Vissers, S., Jauniaux, J.C., van Vliet-Reedijk, J.C., Planta, R.J., and Gibbons, I.R. (1993). Cytoplasmic dynein is required for normal nuclear segregation in yeast. Proc. Natl. Acad. Sci. USA *90*, 11172–11176.

Finger, F.P., and Novick, P. (1998). Spatial regulation of exocytosis: lessons from yeast. J. Cell Biol. *142*, 609–612.

Goosen-de Roo, L., Burggraaf, P.D., and Libbenga, K.R. (1983). Microfilament bundles associated with tubular endoplasmic reticulum in fusiform cells in the active cambial zone of *Fraxinus excelsior*. Protoplasma *116*, 204–208.

Govindan, B., Browser, R., and Novick, P. (1995). The role of Myo2, a yeast class V myosin, in vesicular transport. J. Cell Biol. *128*, 1055–1068.

Hill, K.L., Catlett, N.L., and Weisman, L.S. (1996). Actin and myosin function in directed vacuole movement during cell division in *Saccharomyces cerevisiae*. J. Cell Biol. *135*, 1535–1549.

Kachar, B., and Reese, T.S. (1988). The mechanism of cytoplasmic streaming in *Characea* algal cells: sliding of endoplasmic reticulum along actin filaments. J. Cell Biol. *106*, 1545–1552.

Kilmartin, J.V., and Adams, A.E. (1984). Structural rearrangement of tubulin and actin during the cell cycle of the yeast *Saccharomyces*. J. Cell Biol. *98*, 722–733.

Koning, A.J., Roberts, C.J., and Wright, R.L. (1996). Different subcellular localization of *Saccharomyces cerevisiae* HMG-CoA reductase isozymes at elevated levels corresponds to distinct endoplasmic reticulum proliferations. Mol. Biol. Cell *5*, 769–789.

Lee, C., and Chen, L.B. (1988). Dynamic behavior of endoplasmic reticulum in living cells. Cell *54*, 37–46.

Li, Y.Y., Yeh, E., Hays, T., and Bloom, K. (1993). Disruption of mitotic spindle orientation in a yeast dynein mutant. Proc. Natl. Acad. Sci. USA *90*, 10096–10100.

Lichtscheidl, I.K., Lancelle, S.A., and Hepler, P.K. (1990). Actin-endoplasmic reticulum complexes in *Drosera:* their structural relationship with the plasmalemma, nucleus, and organelles in cells prepared by high pressure freezing. Protoplasma *155*, 116–126.

Liebe, S., and Menzel, D. (1995). Actomyosin-based motility of endoplasmic reticulum and chloroplasts in Vallisneria mesophyll cells. Biol. Cell *85*, 207–222.

Palmer, R.E., Sullivan, D.S., Huffaker, T., and Koshland, D. (1992). Role of astral microtubules and actin in spindle orientation and migration in the budding yeast *Saccharomyces cerevisiae*. J. Cell Biol. *119 583–593*.

Panzner, S., Dreier, L., Hartmann, E., Kostka, S., and Rapoport, T.A. (1995). Posttranslational protein transport in yeast reconstituted with a purified complex of Sec proteins and Kar2p. Cell *81*, 561–570.

Pilon, M., Romisch, K., Quach, D., and Schekman, R. (1998). Sec61p serves multiple roles in secretory precursor binding and translocation into the endoplasmic reticulum membrane. Mol. Biol. Cell *9*, 3455–3473.

Preuss, D., Mulholland, J., Kaiser, C.A., Orlean, P., Albright, C., Rose, M.D., Robbins, P.W., and Botstein, D. (1991). Structure of the yeast endoplasmic reticulum: localization of E.R. proteins using immunofluorescence and immunoelectron microscopy. Yeast *7*, 891–911.

Prinz, W.A., Grzyb, L., Veenhuis, M., Kahana, J.A., Silver, P.A., and Rapoport, T.A. (2000). Mutants affecting the structure of the cortical endoplasmic reticulum in *Saccharomyces cerevisiae.* J. Cell Biol. *150*, 461–474.

Quader, H., Hofmann, A., and Schnepf, E. (1987). Shape and movement of the endoplasmic reticulum in epidermis cells: possible involvement of actin. Eur. J. Cell Biol. *44*, 17–26.

Rose, M.D., Misra, L.M., and Vogel, J.P. (1989). *KAR2*, a karyogamy gene, is the yeast homologue of the mammalian Bip/GRP78 gene. Cell *57*, 1211–1221.

Rossanese, O.W., Soderholm, J., Bevis, B.J., Sears, I.B., O'Connor, J., Williamson, E.K., and Glick, B.S. (1999). Golgi structures correlate with transitional endoplasmic reticulum organization in *Pichia pastoris* and *Saccharomyces cerevisiae.* J. Cell Biol. *145*, 69–81.

Shaw, S.L., Maddox, P., Skibbens, R.V., Yeh, E., Salmon, E.D., and Bloom, K. (1998). Nuclear and spindle dynamics in budding yeast. Mol. Biol. Cell *9*, 1627–1631.

Shaw, S.L., Yeh, E., Maddox, P., Salmon, E.D., and Bloom, K. (1997). Astral microtubules growth/shrinkage in yeast: a microtubule-based searching mechanism for spindle orientation and nuclear migration into the bud. J. Cell Biol. *139*, 985–994.

Sherman, F. (1991). Getting started with yeast. Methods Enzymol. *194*, 3–21.

Simon, V.R., Karmon, S.L., and Pon, L.A. (1997). Mitochondrial inheritance: cell cycle and actin cable dependence of polarized mitochondrial movements in *Saccharomyces cerevisiae.* Cell Motil. Cytoskeleton *37*, 199–210.

Simon, V.R., Swayne, T.C., and Pon, L.A. (1995). Actin-dependent mitochondrial motility in mitotic yeast and cell-free systems: identification of a motor activity on the mitochondrial surface. J. Cell Biol. *130*, 345–354.

Smith, M.G., Simon, V.R., O'Sullivan, and Pon, L.A. (1995). Organelle-cytoskeletal interactions: actin mutations inhibit meiosis-dependent mitochondrial rearrangement in the budding yeast *Saccharomyces cerevisiae.* Mol. Biol. Cell *6,* 1381–1396.

Stevens, B. (1977). Variation in number and volume of the mitochondria in yeast according to growth conditions: a study based on serial sectioning and computer graphics reconstruction. Biol. Cell. *28*, 37–56.

Sullivan, D.S., and Huffaker, T.C. (1992). Astral microtubules are not required for anaphase B in *Saccharomyces cerevisiae.* J. Cell Biol. *119*, 379–388.

Takizawa, P.A., Sil, A., Swedlow, J.R., Herskowitz, I., and Vale, R.D. (1997). Actin-dependent localization of an RNA encoding a cell-fate determinant in yeast. Nature *389*, 90–93.

Terasaki, M., Chen, L.B., and Fujiwara, K. (1986). Microtubules and the endoplasmic reticulum are highly interdependent structures. J. Cell Biol. *103*, 1557–1568.

Tirnauer, J.S., O'Toole, E., Berrueta, L., Bierer, B.E., and Pellman, D. (1999). Yeast Bim1p promotes the G1-specific dynamics of microtubules. J. Cell Biol. *145*, 993–1007.

Tran, P.T., Maddox, P., Chang, F., and Inoue, S. (1999). Dynamic confocal imaging of interphase and mitotic microtubules in the fission yeast *S. pombe*. Biol. Bull. *197*, 262–263.

Waterman-Storer, C., and Salmon, E.D. (1998). Endoplasmic reticulum membrane tubules are distributed by microtubules in living cells using three distinct mechanisms. Curr. Biol. *8*, 798–806.

White, R.G., Badelt, K., Overall, R.L., and Vesk, M. (1994). Actin associated with plasmodesmata. Protoplasma *180*, 169–184.

Yang, H.C., Palazzo, A., Swayne, T.C., and Pon, L.A. (1999). A retention mechanism for distribution of mitochondria during cell division in budding yeast. Curr. Biol. *9*, 1111–1114.

Yeh, E., Skibbens, R.V., Cheng, J.W., Salmon, E.D., and Bloom, K. (1995). Spindle dynamics and cell cycle regulation of dynein in the budding yeast *Saccharomyces cerevisiae*. J. Cell Biol. *130,* 687–700.